FAST UV FLUORESCENCE-BASED IMAGE ANALYSIS FOR PET STAIN LOCALIZATION

TECHNICAL REPORT

Spencer CW Au
Fowler School of Engineering
Chapman University
Orange, CA 92866
spau@chapman.edu

CS615 - Digital Image Processing
Dr. Mohamed Allali

May 23, 2025

ABSTRACT

This study presents a real-time UV (ultraviolet)-based method for detecting pet stains, such as cat urine or hairballs, using only lightweight image processing. By illuminating surfaces with UV light to induce fluorescence, our approach sidesteps the inaccuracy and time overhead of visual inspection or chemical tests, as well as the computational cost of deep learning models. After pre-processing to isolate the UV-illuminated region, surface-adaptive masks branch by background: carpet uses a single Excess Green mask, while wood employs a variety of complementary filters to extract distinct shape information. The masks are then fused into a binary image that highlights biological residues in white. Experimental results demonstrate a fast, reliable, and low-cost solution for pet owners, with broader applications in detection and monitoring systems.

Keywords uv imaging · fluorescence · thresholding · image processing · pet care

1 Introduction

In recent years, there has been a growing integration of image processing technologies into everyday life, leading to advancements in non-invasive detection methods. One of these techniques is UV fluorescence, which has proven to be highly effective for detecting a variety of substances in different fields such as agriculture, forensics, and medical imaging. The purpose of this paper is to document the application of this UV method, specifically by using UV fluorescence to detect cat urine. The motivation behind this application is to address a practical and relevant problem that many pet owners face. Current methods for detecting cat urine, such as relying on visual inspection or chemical tests, can be time consuming and often inaccurate. By leveraging UV light to induce fluorescence and employing image processing techniques to analyze the results, this study aims to provide a more efficient and accurate solution to this issue.

1.1 Literature Review

The concept of ultraviolet (UV) fluorescence for substance detection is not new, and several studies have demonstrated its effectiveness in a variety of fields. A study by Reyes et al. [1] on the detection of mango disease used UV-A light to successfully identify mangoes infected with Anthracnose disease and achieved an accuracy of 94.69% through their computer vision system. This method of UV fluorescence for detecting biological markers shows significant promise for applications of identifying patterns or markers from UV images, which can extend beyond agriculture. Similarly, in forensic investigations, a study by Achetib et al. [2] on fluorescent signatures for body fluid identification showed that body fluids, including urine, exhibit unique fluorescent properties that can be detected with UV fluorescence. This

demonstrates how UV fluorescence can be used to identify substances quickly and non-invasively, which is exactly the approach this paper is exploring here.

As stated previously, the idea of using UV for detection is not limited to agricultural or forensic fields. For example, a study by Giambelluca et al. [3] on scorpion detection combined UV fluorescence with computer vision to detect scorpions based on their shape and fluorescence signatures, achieving an impressive 100% recall rate in detection. Another by Patel et al. [4] reflected UV imaging to detect defects on the surfaces of mangoes, such as bruises and lesions, that would otherwise be invisible under normal lighting. These studies share a common thread about their abilities to use UV light for highly specific detection of biological or physical markers, while remaining non-invasive. They show that UV light can help detect hidden details, whether it is identifying pests or spotting imperfections, and this technique can be adapted for pet urine detection.

Interestingly enough, the techniques proposed in Borhan et al. [5] are similar to the approach we propose taking. Borhan et al. also leverage the HSV color space to detect and segment biological stains. They do opt to use a blue bandpass filter, which transmits only the characteristic 450–490nm fluorescence while blocking both the UV excitation and longer wavelength ambient light, greatly improving contrast. However, high quality optical filters of this type can cost several hundred dollars, making them unjustifiable for our goal of a low cost, lightweight, and real-time system.

The importance of this project comes from the real-world problem of cat urine detection, which is common among pet owners. A system that can quickly and accurately detect these stains is crucial for maintaining a clean home and protecting furniture and flooring. By using simple image processing techniques like converting to grayscale and applying thresholding, this research aims to create a lightweight, computationally efficient system that does not rely on complex deep learning algorithms, making it more accessible for everyday use. This approach aligns with the growing demand for practical, cost-effective solutions to everyday tasks, such as pet care. By offering a more accessible and efficient approach, the findings from this study have the potential to be expanded for broader use in various detection and monitoring systems.

2 Methodology

2.1 Overview

The pipeline adapts to two surface types (wood vs. carpet) and proceeds through four main stages. All image processing is done in MATLAB.

1. Acquire image with fluorescence via UV illumination
2. Perform pre-processing by resizing and isolate the UV-illuminated region via an HSV crop.
3. Apply surface-adaptive masks:
   - Carpet: single Excess-Green mask
   - Wood: complementary filters (ExG, HSV line, Fourier, woodgrain)
4. Fuse all binary masks into a final composite.

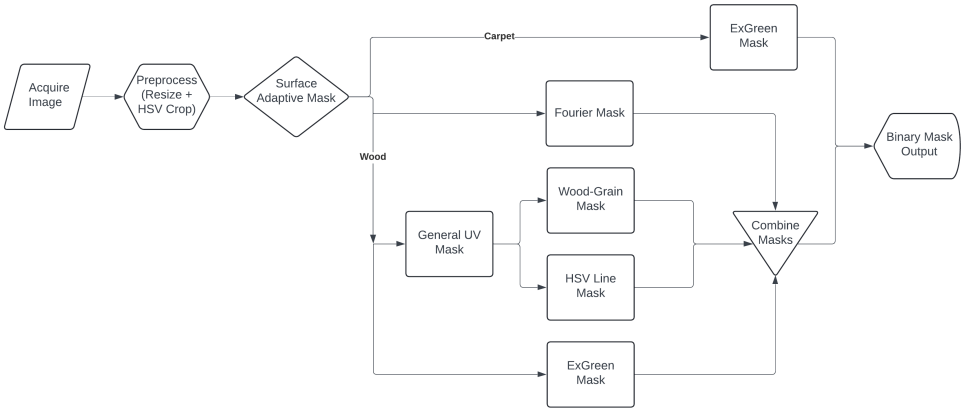

Figure 1: High-level pet-stain detection pipeline with carpet/wood branching.

2.2 Image Acquisition

A proof of concept evaluation was conducted on nine images. Four on bedroom carpet and five on living room wood surfaces. All photographs were captured with the 48 MP camera of an Apple iPhone 15 Pro Max under illumination from a Sofirn SF16 365 nm UV flashlight. The carpet images were captured in near dark conditions, while the wood surface images included ambient light from both exterior sources and interior apartment lighting. Camera settings remained at the iOS default for the camera application.

2.3 Preprocessing

Image Resizing All input images are first passed through a height-based resizer to limit processing cost and ensure consistent scale. Given a maximum height $H_{\max}$, any image taller than $H_{\max}$ is downsampled by a uniform scale factor:

$$s = \frac{H_{\max}}{H_{\text{orig}}}$$

using MATLAB's `imresize`. Images shorter than $H_{\max}$ remain at full resolution. This preserves aspect ratio while bounding the largest dimension. In this specific application, we have chosen to resize the images to 512 pixels.

UV Region Extraction Next, each resized image is converted to the HSV color space and thresholded to isolate the region fluorescing under 365 nm UV light. We form a binary UV mask by selecting pixels with

$$0.55 < Hue < 0.80, \quad Saturation \geq 0.20, \quad Value \geq \mu_V + 0.10,$$

where μ_V is the mean brightness of non-zero pixels. These thresholds were chosen to capture the characteristic blue–violet "beam" of a 365 nm UV flashlight. By limiting Hue to the 0.55–0.80 band to correspond to blue-violet color, enforcing a minimum Saturation to exclude the non illuminated background, and raising the Value cutoff dynamically above the scene's mean brightness, we ensure that only genuinely fluorescent regions are retained. We then keep only the largest connected component, compute its centroid and equivalent diameter, then build a circular mask with a 25 pixel pad around it. Finally, we crop to the bounding box of that circle and zero out everything outside so that all downstream steps operate solely on the UV illuminated region.

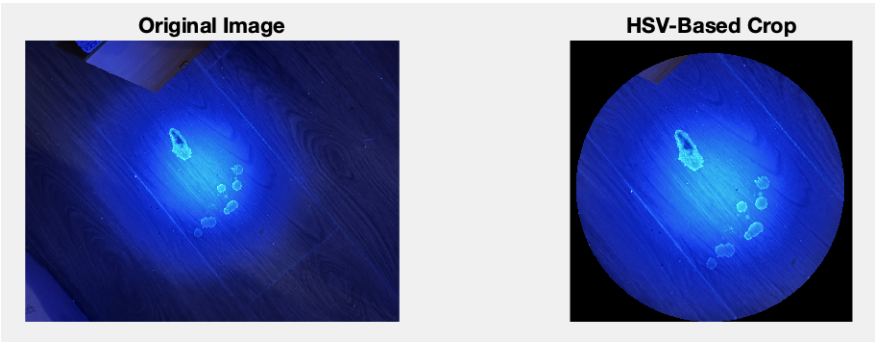

Figure 2: HSV Crop Technique

2.4 Surface-Adaptive Masking

The test images used are of two distinct background surfaces: one being a wood surface with distinctive wood-grain patterns, and the other being a typical bedroom carpet. In addition, the bedroom carpet images seem to be mainly the regurgitated hair biological material with a more distinctive UV fluorescence in contrast to the wood surface, which is comprised of more subtle fluorescent spots. Based on whether the background surface is a carpet or wood image, we either apply a sole ExGreen (Excess Green) mask or a variety of masks respectively.

2.4.1 Bedroom Carpet

On carpet backgrounds, we use a single ExGreen mask in the RGB space. The input image is converted to double precision and the Excess Green index is computed as

$$\text{ExG} \;=\; 2G - R - B.$$

These values are then normalized to [0,1] via the global image minimum and maximum. A threshold is chosen at the top pth percentile of the normalized ExG values (usually the top 90-95% for carpet images), and pixels above this cutoff are retained. The resulting binary mask is refined by a morphological closing with a disk of radius 6 pixels, followed by hole filling, and finally by keeping only connected components of at least 40 pixels.

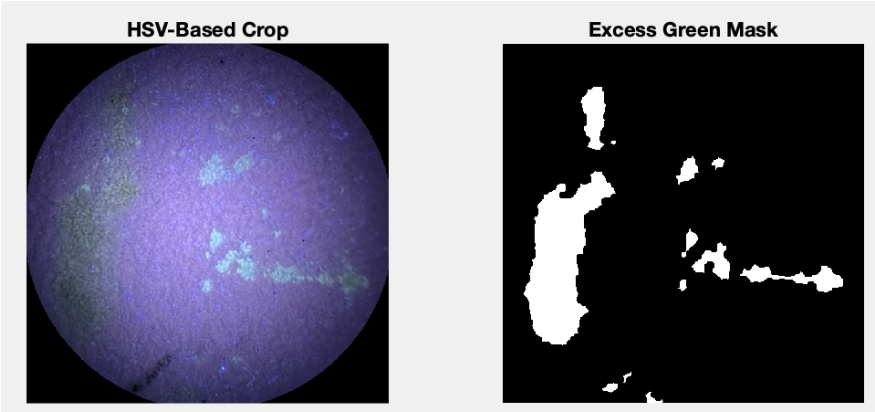

Figure 3: ExGreen Mask with 95% Threshold

2.4.2 Living Room Wood

On wood floors, we generate four complementary masks from the UV-cropped region. The general UV mask is first used to create both the wood-grain filter and HSV line masks, while the Fourier mask, ExGreen mask, and the general UV mask itself are computed directly from the circular UV crop. All masks are then fused by logical OR to produce the final binary output.

General UV Mask The circular UV region crop is converted to grayscale and pre-filtered with a 5×5 median filter to remove noise and contrast is enhanced via adaptive histogram equalization (ClipLimit = 0.01). The image is then binarized using a 25×25 median neighborhood adaptive threshold (sensitivity = 0.45). "Blobs" smaller than 30 pixels are removed, and holes in bright regions are filled.

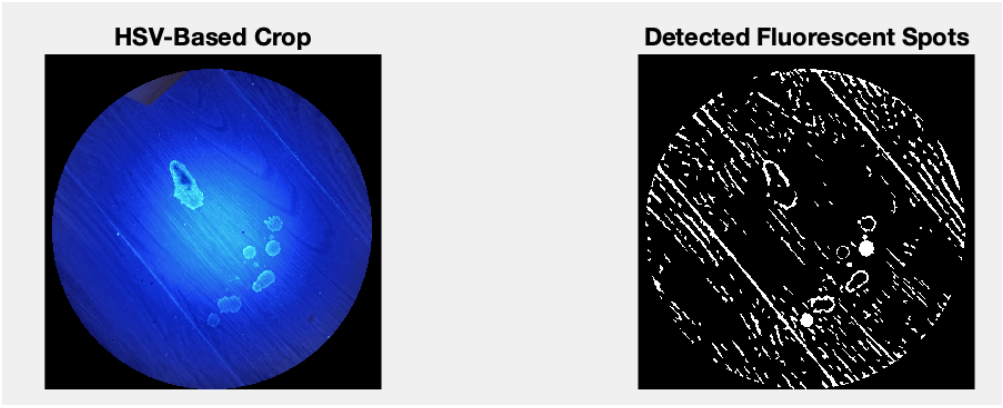

Figure 4: General UV Thresholding Mask

Excess Green Mask The Excess Green mask introduced for carpet surfaces (see Section 2.4.1) is also applied to wood images. The index $\mathrm{ExG} = 2G - R - B$ is normalized to [0,1] and thresholded at the 95-98th percentile to isolate bright fluorescent regions.

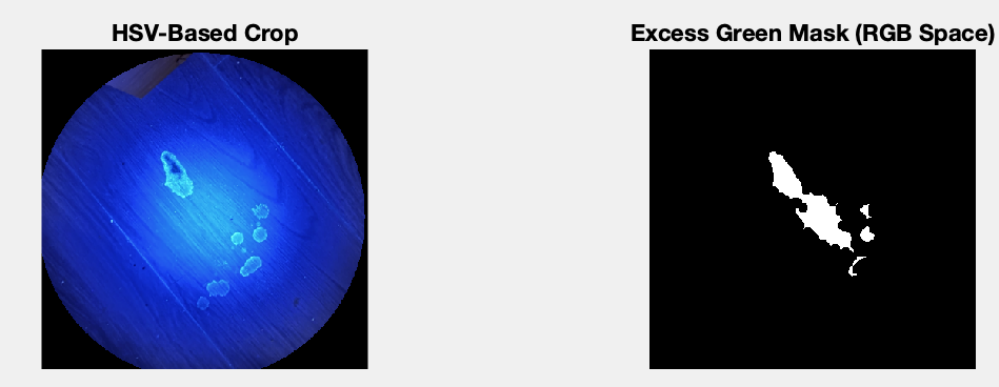

Figure 5: Wood Surface ExGreen Mask with 98% Threshold

Wood-Grain Filter Mask To remove the linear texture of wood-grain patterns, the binary threshold image is processed with a sequence of morphological openings. Five linear structuring elements with a minimum length of 10 pixels are applied at angles of $\pm 15°$, $\pm 30°$, and $120°$. Each opening step suppresses features aligned with its orientation, effectively erasing wood-grain lines while preserving fluorescent spots. The result is a cleaner mask that highlights only the relevant biological residues without highlighting the wood-grain textures.

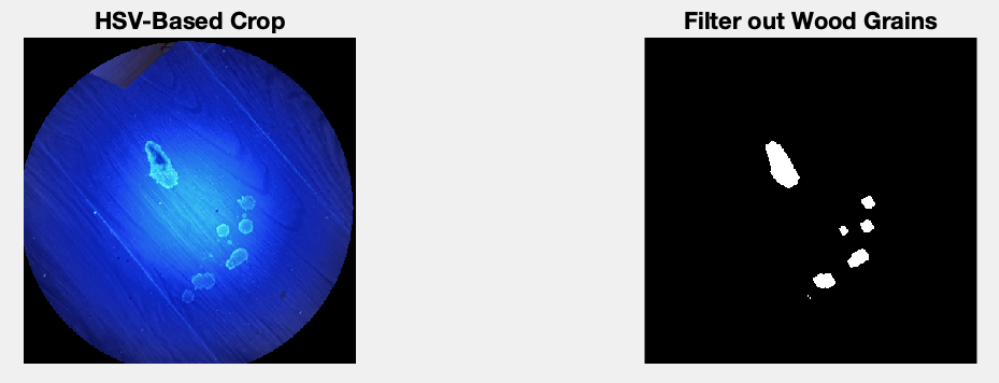

Figure 6: Wood-Grain Filter Mask

Line Mask The threshold image is first skeletonized and labeled. Then, only the components with a minimum length of 170 pixels and an eccentricity of at least 0.99 are retained. The result is dilated by a 1 pixel disk to thicken the lines.

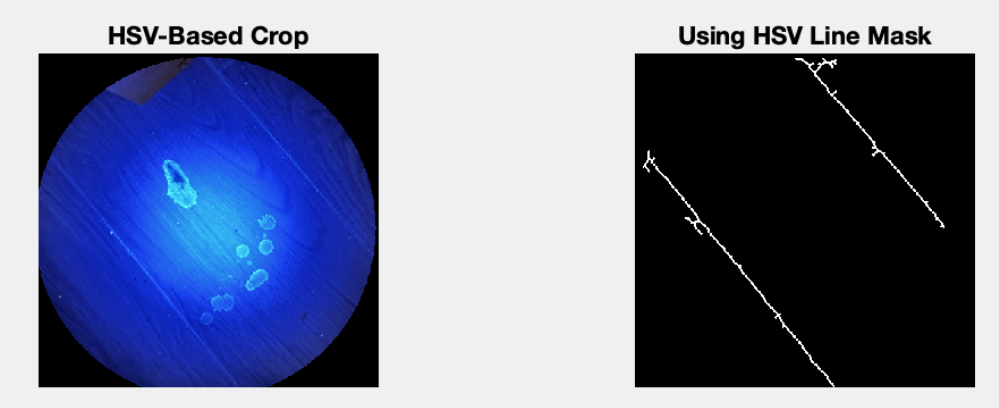

Figure 7: Solid Line Filter Mask

Fourier Mask To highlight fluorescent features and suppress both very fine and very coarse textures, we transform the UV cropped grayscale image into the frequency domain via a 2D Fourier transform. A radial band pass filter selects frequencies around $1/D$ (with $D = 40$ and a bandwidth fraction of 0.5), removing both low-frequency background variations and high-frequency noise. The filtered spectrum is then inverted back to the spatial domain, normalized, and thresholded at 0.7 to produce a binary mask. Finally, we use a 100 pixel border (roughly 10-20% of the input image of 512 pixels) in order to avoid the circular crop ring that "lights up".

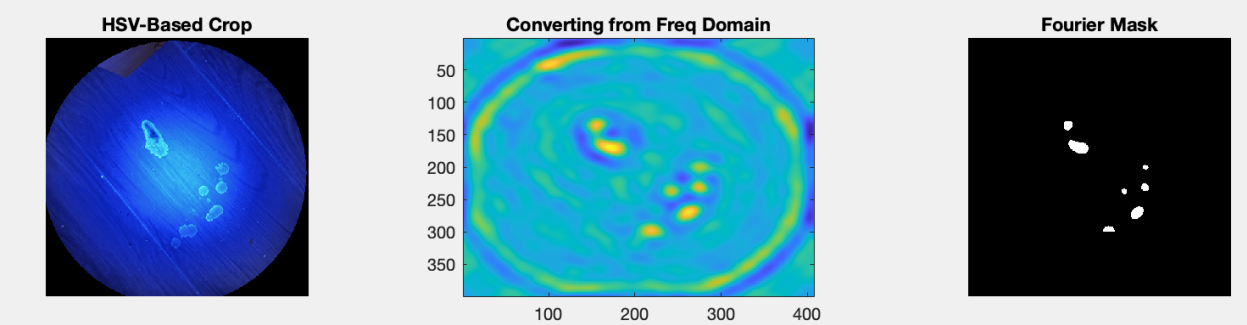

Figure 8: Fourier Mask

2.5 Mask Fusion

If the background surface is the bedroom carpet, then only the Excess Green Mask is necessary to form the final binary output. If the background surface is wood, then the four masks (Wood-Grain Filter, Line Filter, Fourier Mask, and the ExGreen mask from RGB) are combined by logical OR in order to produce the final binary output.

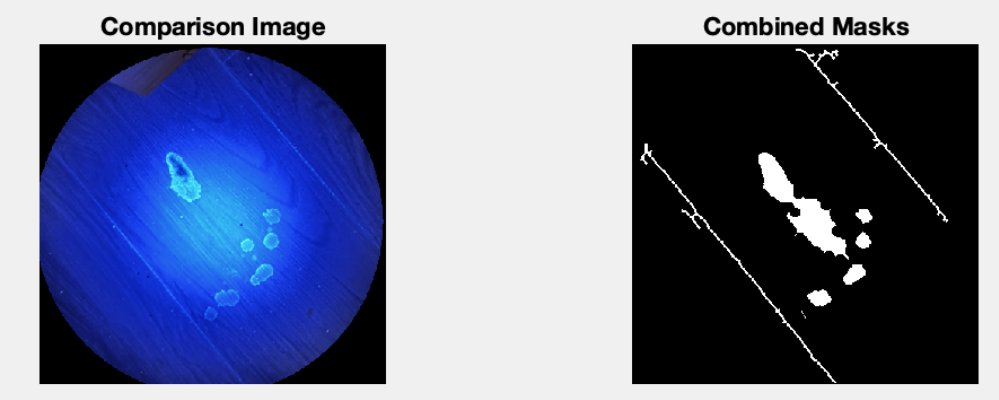

Figure 9: Example Binary Output for Wood Surface

3 Results

3.1 Wood Surface Images

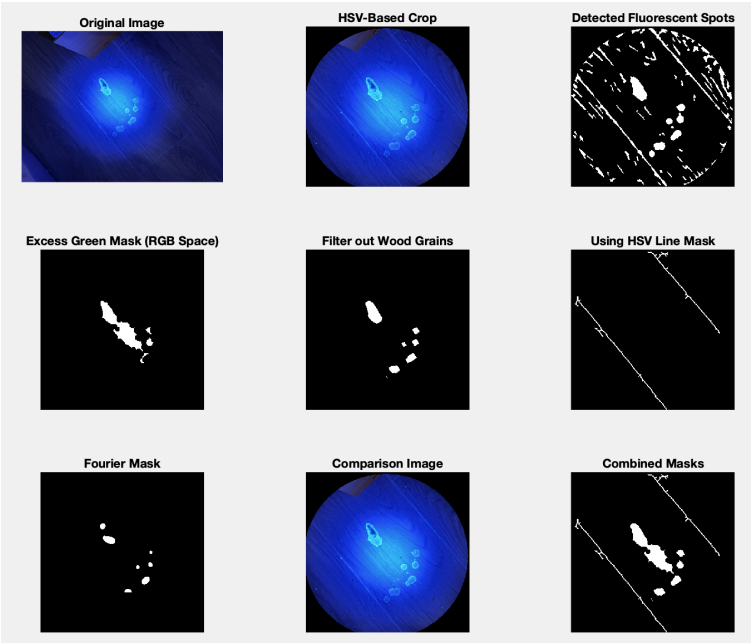

Figure 10: A: Example Binary Output for Wood Surface

In figure 10 above, we can see that the overall approach seems to work decently well at isolating out the UV fluorescent regions. The one issue does seem to be the addition of the ExGreen Mask, which seems to include a portion of the central illuminated region to the final binary output mask.

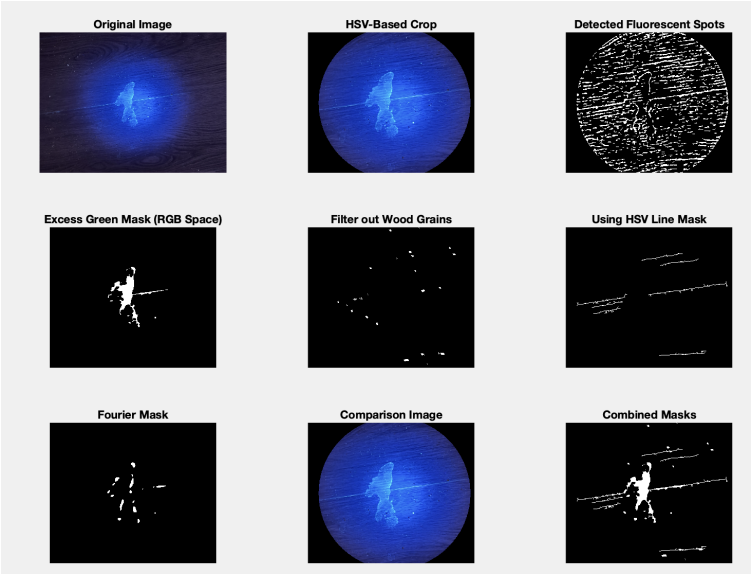

Figure 11: B: Example Binary Output for Wood Surface

In figure 11, we can see a good example of why it is necessary to include the ExGreen mask when processing images on the wood surface background. While the Fourier mask does seem to include the rough general shape of the center "blob", the ExGreen mask performs the best at catching this particular type of biological stain.

3.2 Carpet Surface Images

Carpet images offer clearer fluorescence contrast, likely because hair regurgitation emits stronger green fluorescence under UV and ambient light was minimal. Consequently, a simple ExGreen mask in the RGB color space suffices to identify stained regions.

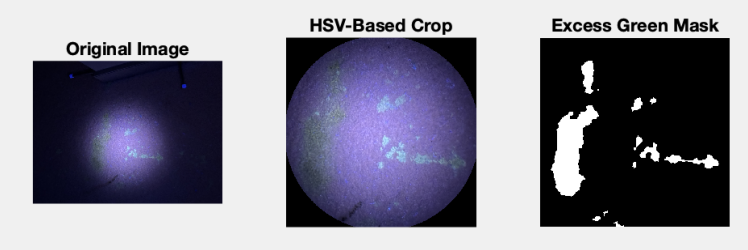

Figure 12: A: Example Binary Output for Carpet Surface

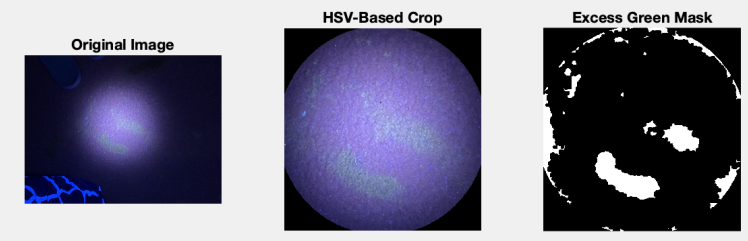

Figure 13: B: Example Binary Output for Carpet Surface

4 Discussion

Overall, this approach seems to be fairly successful, while still adhering to traditional digital image processing techniques. The processing speed is sufficiently fast for real-time and embedded applications, in contrast to many modern machine learning approaches. Because our filters and thresholds are hand tuned, every step is transparent. A user can view intermediate masks, see why any pixel was kept or removed, and tweak one parameter at a time. Debugging is as simple as changing a value and rerunning, and results stay predictable without any retraining.

The next phase begins by refactoring the MATLAB scripts into a fully modular library, parameterizing every threshold, structuring element size, and dimensional constant rather than leaving them hard-coded. Once the API is stable, MATLAB Coder will export ANSI C source code, which we compile into a shared library (such as a .dll). We will also use Valgrind (or equivalent tools, especially for MacOS ARM64 architectures) to profile memory usage, eliminate leaks, and optimize performance at the C level. That library will then be packaged as a Python wheel, linking directly against the compiled C code, so that all routines may be called from Python with minimal overhead. This workflow leverages the existing MATLAB generated C code for maximum performance, simplifies deployment via a standard pip install, and keeps the core algorithms synchronized in one codebase.

After Python integration, we will deploy the system on a microcontroller (for example, a Raspberry Pi) as a lightweight, ceiling mounted unit with a downward facing camera. The floor will be divided into M blocks, each covering an N x N area. Whenever the detected biological fluorescence in any block exceeds a predefined threshold, the system will trigger a response, such as sending an alert or dispatching an automated cleaner equipped with an enzyme sprayer, to that respective block's location.

Code Availability

The full source code for this project is freely available on GitHub at UV_SpotDetection and is covered under the GNU Affero General Public License Version 3.0.

References

[1] Abigail M. Delos Reyes, Daryl Khent A. Lorzano, John Francis S. Madrigal, and Mark Angelo C. Purio. Uv-based computer vision system for early detection and segregation of mango anthracnose disease. *2023 IEEE 15th International Conference on Humanoid, Nanotechnology, Information Technology, Communication and Control, Environment, and Management (HNICEM)*, pages 1–6, 11 2023. doi:10.1109/hnicem60674.2023.10589025. URL https://www.researchgate.net/publication/382278898_UV-Based_Computer_Vision_System_for_Early_Detection_and_Segregation_of_Mango_Anthracnose_Disease.

[2] Nihad Achetib, Kim Falkena, Meghna Swayambhu, Maurice C. G. Aalders, and Annemieke van Dam. Specific fluorescent signatures for body fluid identification using fluorescence spectroscopy. *Scientific Reports*, 13:3195, 02 2023. doi:10.1038/s41598-023-30241-7. URL https://www.nature.com/articles/s41598-023-30241-7.

[3] Francisco Luis Giambelluca, Jorge R Osio, Luis A Giambelluca, and Marcelo A Cappelletti. Novel scorpion detection system combining computer vision and fluorescence. *arXiv (Cornell University)*, 01 2021. doi:10.48550/arxiv.2108.04177.

[4] Krishna Kumar Patel, A. Kar, and M. A. Khan. Potential of reflected uv imaging technique for detection of defects on the surface area of mango. *Journal of Food Science and Technology*, 56:1295–1301, 02 2019. doi:10.1007/s13197-019-03597-w.

[5] Nuradlin Borhan, Azwati Azmin, Masaki Yamakita, and Wan Mohd. Biological stain detection using opencv with the aid of ultraviolet a (uva) light. *ASEAN Engineering Journal*, 13:65–70, 08 2023. doi:10.11113/aej.v13.19064.

[6] Jiaqi Song, Baolei Liu, Yao Wang, Chaohao Chen, Xuchen Shan, Xiaolan Zhong, Ling-An Wu, and Fan Wang. Computational and dark-field ghost imaging with ultraviolet light. *Photonics Research*, 12:226–226, 11 2023. doi:10.1364/prj.503974.

[7] Wei Li, Qinyong Lin, Keqiang Wang, and Ken Cai. Machine vision-based network monitoring system for solar-blind ultraviolet signal. *Computer Communications*, 171:157–162, 03 2021. doi:10.1016/j.comcom.2021.03.014.

[8] Hary Kurniawan, Muhammad, Santosh Lohumi, Moon S Kim, Insuck Baek, and Byoung-Kwan Cho. Dual imaging technique for a real-time inspection system of foreign object detection in fresh-cut vegetables. *Current Research in Food Science*, 9:100802–100802, 01 2024. doi:10.1016/j.crfs.2024.100802.

[9] Thomas G Kaye and Michael Pittman. Fluorescence-based detection of field targets using an autonomous unmanned aerial vehicle system. *Methods in Ecology and Evolution*, 11:890–898, 06 2020. doi:10.1111/2041-210x.13402.

[10] Qibin Zhuang, Yankun Peng, Deyong Yang, Sen Nie, Qinghui Guo, Yali Wang, and Renhong Zhao. Uv-fluorescence imaging for real-time non-destructive monitoring of pork freshness. *Food Chemistry*, 396:133673, 12 2022. doi:10.1016/j.foodchem.2022.133673.

[11] Brijen Thananjeyan, Justin Kerr, Huang Huang, Joseph E Gonzalez, and Ken Goldberg. All you need is luv: Unsupervised collection of labeled images using uv-fluorescent markings. *2022 IEEE/RSJ International Conference on Intelligent Robots and Systems (IROS)*, 10 2022. doi:10.1109/iros47612.2022.9981768.

[12] Syed Raza Mehdi, Kazim Raza, Hui Huang, Rizwan Ali Naqvi, Amjad Ali, and Hong Song. Combining deep learning with single-spectrum uv imaging for rapid detection of hnss spills. *Remote Sensing*, 14:576, 01 2022. doi:10.3390/rs14030576.

[13] Marc Köntges, Arnaud Morlier, Gabriele C Eder, Eckhard Fleis, Bernhard Kubicek, and Jiang Lin. Review: Ultraviolet fluorescence as assessment tool for photovoltaic modules. *IEEE Journal of Photovoltaics*, 10:616–633, 01 2020. doi:10.1109/jphotov.2019.2961781.

[14] Hong-xia Li, Jing Cao, Jie-qing Niu, and Yun-gang Huang. Study of uv imaging technology for noninvasive detection of latent fingerprints. *SPIE Proceedings*, 8905:89051L, 09 2013. doi:10.1117/12.2034451.

[15] Mitchell Sueker, Kristen Stromsodt, Hamed Taheri Gorji, Fartash Vasefi, Nadeem A Khan, Taylor Schmit, Rangati Varma, Nicholas B Mackinnon, Stanislav V Sokolov, Alireza Akhbardeh, Bo Liang, Jianwei Qin, Diane E Chan, Insuck Baek, Moon S Kim, and Kouhyar Tavakolian. Handheld multispectral fluorescence imaging system to detect and disinfect surface contamination. 21:7222–7222, 10 2021. doi:10.3390/s21217222.

[16] Ron Cooper and Okan Caglayan. Development of a hybrid ultraviolet imaging algorithm for optical sensing systems. 03 2021. doi:10.18260/1-2–36372.

[17] Ying Wang, Enoch Gutierrez-Herrera, Antonio Ortega-Martinez, Richard Rox Anderson, and Walfre Franco. Uv fluorescence excitation imaging of healing of wounds in skin: Evaluation of wound closure in organ culture model. *Lasers in Surgery and Medicine*, 48:678–685, 09 2016. doi:10.1002/lsm.22523. URL https://pubmed.ncbi.nlm.nih.gov/27075645/.